BSENSE: In-vehicle Child Detection and Vital Sign Monitoring with a Single mmWave Radar and Synthetic Reflectors

Mingyue Tang, Pranshu Teckchandani, Jizheng He, Hanbo Guo, Elahe Soltanaghai
University of Illinois, Urbana-Champaign
Urbana-Champaign, USA
{mt55,pat4,jizheng4,hanbog2,elahe}@illinois.edu

Abstract

Recent regulations on monitoring infants and children in vehicle cabins have spurred interest in using Millimeter-wave (mmWave) radars due to their reliability in various lighting conditions and privacy benefits. However, existing radar-based vital sign detection solutions fail in car settings with abundant occlusions or closely-seated multi-person scenarios. To resolve these limitations, we introduce BSENSE, a joint occupancy and vital sign monitoring system using a single radar that is robust to occlusion and varying seating arrangements and number of occupants in vehicle cabins. BSENSE incorporates synthetic wireless reflectors positioned in car corners to redirect radar signals toward blind spots, enabling Non-Line-of-Sight (NLoS) vital sign detection while maintaining sensing performance in Line-of-Sight (LoS) areas. The proposed system employs a hybrid architecture combining signal processing and a deep learning pipeline that can detect the car seating layout and jointly learn occupied seats and signatures of breathing to distinguish adults from children and infants, and monitor their vital signs over time. Our extensive evaluations with 120,000 radar data points, 400 different experimental scenarios, a mix of 10 adults, 5 children of age 1-11, and two programmable infant and child simulators demonstrate BSENSE's capability in child detection with over 97% accuracy and estimating their breathing rate within 6 BPM error, even in multi-person and NLoS scenarios, and across different car models.

CCS Concepts

• **Human-centered computing** → **Ubiquitous and mobile computing systems and tools**; • **Computing methodologies** → **Machine learning**; • **Hardware** → **Analysis and design of emerging devices and systems**.

Keywords

Child Presence Detection, Millimeter Wave, SFCW, Synthetic Reflector, Vital Sign Detection

ACM Reference Format:
Mingyue Tang, Pranshu Teckchandani, Jizheng He, Hanbo Guo, Elahe Soltanaghai. 2024. BSENSE: In-vehicle Child Detection and Vital Sign Monitoring with a Single mmWave Radar and Synthetic Reflectors. In *ACM Conference on Embedded Networked Sensor Systems (SenSys '24), November 4–7, 2024, Hangzhou, China.* ACM, New York, NY, USA, 15 pages. https://doi.org/10.1145/3666025.3699352

SenSys '24, November 4–7, 2024, Hangzhou, China

ACM ISBN 979-8-4007-0697-4/24/11
https://doi.org/10.1145/3666025.3699352

1 Introduction

In the past decades, forgotten infants have been the majority cause (an average of 53%) of juvenile heatstroke deaths in cars [19]. Children's core temperature increases three to five times faster than adults [8], taking only a few minutes for the temperature inside a car to reach levels that can result in such severe consequences. However, this is not the only scenario where infants face life-threatening dangers inside a vehicle's cabin. Recent research has revealed a link between car seats and Sudden Infant Death Syndrome (SIDS) [64] due to breathing difficulties when they are in a seated position for too long, typically while sleeping. These situations could happen even when children are accompanied by adults in the car during long drives. Therefore, only detecting the presence of unattended children in a parked car is insufficient to build a reliable in-vehicle infant monitoring system.

Researchers and industry have attempted various child presence detection (CPD) systems with different sensors. This includes pressure/weight sensors [30], carbon dioxide sensors [86], ultrasonic sensors [28], passive infrared sensors [41], cameras [85], acoustics [22, 37, 72, 87, 107], WiFi systems [46, 103], or radars [14, 57, 59, 69, 84, 90, 95]. However, these solutions either suffer from sensitivity to temperature and lighting variations (e.g. CO_2, and infrared sensors), assume a designated position (e.g. pressure sensors), or only work in the Line-of-Sight (LoS) (e.g. camera sensors). While wireless-based solutions including acoustic, WiFi and radar are theoretically robust to these conditions, the existing radar-based solutions either lack vital sign detection capability [9, 84] or fail in multi-person scenarios or rear-facing conditions [14, 18, 38, 90, 108] due to the high dynamic signal range.

The core challenge in detecting infants in cars arises from the changing orientation of their car seats as they grow, which presents significant hurdles for sensor placement and data interpretation. Based on National Highway Traffic Safety Administration regulations, children under two years old or 40 pounds are mandated to have a rear-facing seat [2]. Once a child outgrows the rear-facing seat, they transition to a forward-facing car seat with a harness. In addition, some countries and even states in the US allow car seats in the front passenger seat [10], while others not. As such, there is no single sensor position that can cover all rows or car seat orientations. One naive approach to address this is to equip the car with multiple sensors (e.g., one radar for each row), but that significantly escalates both the cost and potential signal interference.

To address these limitations, we present BSENSE, an in-vehicle contactless child occupancy and vital sign detection system using

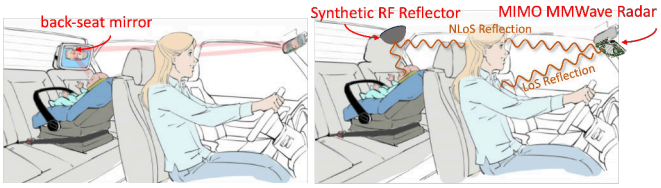

(a) manual visual-based infant monitoring (b) RF-equivalent of back-seat mirror

Figure 1: BSENSE leverages built-in synthetic reflectors in corners of car cabins to mimic the back-seat mirrors for radars, enabling infant presence, location, and vital sign detection even in rear-facing positions.

a single Stepped-Frequency Continuous Wave (SFCW) millimeter-wave (mmWave) radar that can differentiate adults from infants and children by combining seat occupancy and the standard respiration rates for different ages [76]. The SFCW waveform of the radar offers the flexibility of increasing SNR in short ranges without compromising signal resolution. The mmWave frequency offers high phase sensitivity due to the shorter wavelengths. These properties allow mmWave radars to detect small displacements with remarkable precision, such as the subtle chest movements of an infant due to breathing. In addition, BSENSE uses a single mmWave radar placed in front of the car, which offers simplified installation without the need for complex wiring and expands the radar coverage using passive synthetic Radio Frequency (RF) reflectors in the corners of the car. In essence, BSENSE uses the law of scattering from convex surfaces [34] to passively redirect the signals to the radar blind spots without affecting the sensing performance in LoS areas, similar in context to back-seat mirrors but for the radar (shown in Figure 1). As such, BSENSE is robust to different orientations or positions, even if the infant is in a rear-facing car seat covered with a blanket or in the presence of multiple people in the car. BSENSE not only satisfies the European New Car Assessment regulations [106] on child presence detection but also provides continuous monitoring of a child's wellness in the car, offering peace of mind for the parent driving the car.

With the use of passive reflectors, we can ensure reception of a reflection from NLoS areas. However, distinguishing the weak reflections from the infant's body in the presence of one or multiple adults or other moving objects with larger Radar Cross Section (RCS) is still very challenging. To overcome these challenges, BSENSE introduces a hybrid architecture that combines signal processing and deep learning to jointly capture the body volume for occupancy detection as well as breathing recordings for vital sign detection. The pipeline consists of spatio-spectral and temporal filters that capture the physics of RF propagation and the periodic but varying nature of human respiration in car environments. BSENSE processing architecture consists of three main components:

- **4D Spatial-Phase Beamforming:** BSENSE's first component uses a combination of 4D FFT and phase beamforming to focus on regions with the highest likelihood of reflections from the occupant's body and convert raw radar data into spatial and spectral features within 3D car space. We demonstrate that this hybrid FFT and beamforming method can effectively extract and distinguish weak reflections from infants' bodies from strong reflections of adults, even in NLoS scenarios.
- **Joint Occupancy & Vital Sign Learning:** This component translates spectral and spatio-temporal features extracted from RF reflections into seat occupancy and their corresponding breathing rates. BSENSE presents a joint learning framework that employs occupancy and vital sign models as constraints for each other. This is achieved through a two-fold radar embedding and multi-task modeling approach.
- **Automatic Adaptation to New Car Models:** The final component of BSENSE's processing pipeline is a transfer learning algorithm that adapts the occupancy and vital sign task heads to new car layouts and sizes. The component utilizes the learned embeddings with underlying occupancy and respiration features but fine-tunes the multi-task prediction models using a small amount of annotated data during radar deployment. The BSENSE two-fold neural architecture allows us to significantly reduce the required training data for adaptation to new environments.

We prototype an end-to-end system using IMAGEVK-74 millimeter radar board from Vayyar [9] with 20 transmitting vertical antenna elements and 20 receiving horizontal elements that operate with SFCW waveform in 62-66.5 GHz band. We first recruit 10 adults and use an infant and child simulator with programmable respiration rate and various body movements to systematically evaluate BSENSE under various conditions both in indoor environments and in cars. Then, we conduct a real-world study with 5 children, aged 1 to 11 for testing in various cars. Our results from 120,000 radar data points across 400 different experimental scenarios with leave-one-out testing show that BSENSE archives an overall child detection rate of 97% and can monitor their vital signs with an average of 6 Breaths-Per-Minute (6 BPM) with or without the presence of adults in the car. BSENSE also preserves its high performance in NLoS and rear-facing infant settings.

Contributions: our core technical contributions are:

- A novel design of a mmWave sensing platform for infant detection inside vehicles through a bundle of single mmWave radar and carefully designed synthetic reflectors for covering radar blind spots and NLoS areas.
- A hybrid signal processing and deep learning algorithm for joint occupancy and vital sign learning, which enables infant presence detection, unattended child detection, and wellness monitoring over time, even in the presence of adults in the car.
- A detailed system implementation and evaluation in varied settings, including various car sizes and real children.

Code available at: https://github.com/mtang724/BSENSE-in-cabin/.

2 Design Space

In this section, we first define the challenges of radar-based in-vehicle infant monitoring and why previous radar solutions for health monitoring or occupancy detection are not applicable. Next, we explain our reasoning for the choice of SFCW mmWave radars and its placement in the car.

2.1 Why Is Infant Monitoring Challenging?

One of the main challenges in child and infant monitoring with radars is the weak reflected signals from their bodies due to their low Radar Cross Section (RCS) compared to adults or even the surrounding environment. Previous works [13, 16] have employed

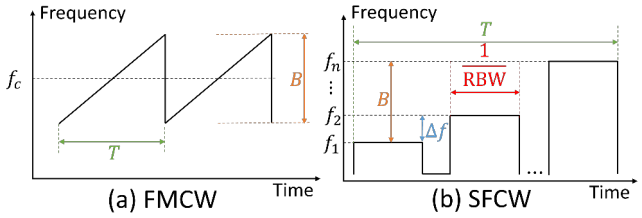

Figure 2: Popular radar signal waveforms.

various background and clutter removal techniques such as the Constant False Alarm Rate (CFAR) algorithm [58] to address this issue. Subsequently, features like range, angle, and radar point clouds are used for in-vehicle occupancy detection [52, 80]. However, infants' movements especially in NLoS scenarios are too subtle to be detected by commodity mmWave radars. Alternatively, the digital beamforming techniques [38] can enhance the signal-to-noise ratio. However, this approach requires pre-defining the target distance to the radar, which is not applicable to car settings with varying sizes and infant positions [60].

Another common technique for infant monitoring is the detection of body micro-movements due to breathing or heart activities. The periodic nature of these movements creates a non-zero Doppler frequency for the radar reflections from the chest. However, Doppler-based methods are prone to false alarms triggered by the movement of other objects. Moreover, unrelated movements of the person can mask the Doppler information related to vital signs. As such, Doppler-based methods are mainly used in static cases, such as sleep monitoring or controlled setups when the user is sitting still in front of the radar [38].

2.2 Why SFCW Millimeter-wave Radars?

While the majority of previous radar-based vital-signs detection research [14, 18, 36, 38, 90, 96, 108] is based on Frequency-Modulated Continuous-Wave (FMCW) radars, BSENSE utilizes Stepped-Frequency Continuous-Wave (SFCW) radar systems. SFCW radars have a distinct advantage in short-range applications compared to FMCW. The main difference between these two radar systems lies in the transmitted signal waveform: unlike FMCW radars that transmit chirps with linearly increasing frequency, SFCW radars emit continuous waves with frequencies that increment in predefined steps with equal frequency differences (Figure 2). At each frequency step, an SFCW radar transmits a constant frequency tone for a time duration inversely proportional to the resolution bandwidth (RBW). This duration allows the oscillator circuit to fully saturate and transmit a stable monocromatic wave. It then samples and averages across multiple received signals at that frequency to provide a frequency response robust to hardware noise. Furthermore, RBW can be decreased to stay at each step for a longer duration, resulting in a higher signal-to-noise ratio (SNR) without affecting the range resolution. This is suitable for in-vehicle sensing that requires the detection of weak reflections at relatively short ranges without sensing targets outside of the boundary of the cabin.

To explain why this is an advantange specific to SFCW radars, let us compare the range resolution and maximum unambiguous range equations for both waveforms:

$$R_{\text{res}}^{\text{FMCW}} = R_{\text{res}}^{\text{SFCW}} = \frac{c}{2B} \tag{1}$$

$$R_{\text{max}}^{\text{FMCW}} = \frac{c}{2B} \cdot N_s \qquad R_{\text{max}}^{\text{SFCW}} = \frac{c}{2\Delta f} = \frac{c}{2B} \cdot N_{\text{step}} \tag{2}$$

where c is the speed of light, B is the bandwidth, N_s is the FMCW sample number per chirp, Δf is the SFCW step frequency difference, and N_{step} is the number of steps per SFCW frame. In SFCW, the step duration can be increased to achieve higher SNR while having no effect on the range resolution and maximum range since N_{step} is kept constant. However, in FMCW, with the same sampling frequency, longer chirp duration increases the number of samples N_s, which consequently increases the maximum range and becomes abundant for near-range sensing in in-cabin scenarios. Since FMCW chirps linearly increases its transmitting frequency, one cannot simply take windowed averages on FMCW samples to improve SNR. This poses additional hardware and processing requirements on handling larger amounts of samples. In short, SFCW radar has the flexibility in choosing the duration of staying at each frequency in favor of higher signal gain for short-range applications.

2.3 Where to Install the Radar in the Car?

A key challenge in using mmWave radars for in-vehicle sensing is the abundance of NLoS areas where the radar's emitted signal cannot reach the target. For example, children under two years old are mandated to have rear-facing car seats. On the other hand, the front row seats may block small children or adults sitting in the back seats. Previous works have examined different radar locations for in-vehicle sensing, such as under the rear-view mirror in front of the car for driver monitoring [47, 89], under the car roof in the middle for occupancy detection [15], or on the roof in the back row for infant monitoring [14]. However, there is no single position to install the radar that can cover all rows and work for both occupancy detection and vital sign detection of driver, infants, or passenger adults and children in the car. One naive solution is to install multiple radars in the car, such as one for each row, but that significantly escalates both the cost and signal interference issues. To address this problem, we propose to place the radar in front of the cabin under the rear mirror, which is also the ideal position for wiring and access to the electronic control unit in the car, and place a set of synthetic reflectors at the corners of the cabin to help the transmitted signal reach NLoS areas, shown in Figure 6. Given the increasing interest from car manufacturers in radar-based in-cabin monitoring systems [4, 92], these reflectors can be seamlessly integrated into the vehicle's interior framework during car manufacturing. This integration incurs negligible cost overhead, eliminating the need for individuals to install the reflectors separately and thereby avoiding additional expenses. In the next sections, we elaborate on the design of synthetic reflectors and their placements in the car.

3 BSENSE System Design

An overview of BSENSE system is depicted in Figure 3. BSENSE receives the raw IQ data from multiple transmitting and receiving antennas of a single-chip radar and jointly estimates seat occupancy and respiration rates, which will be then used child detection or

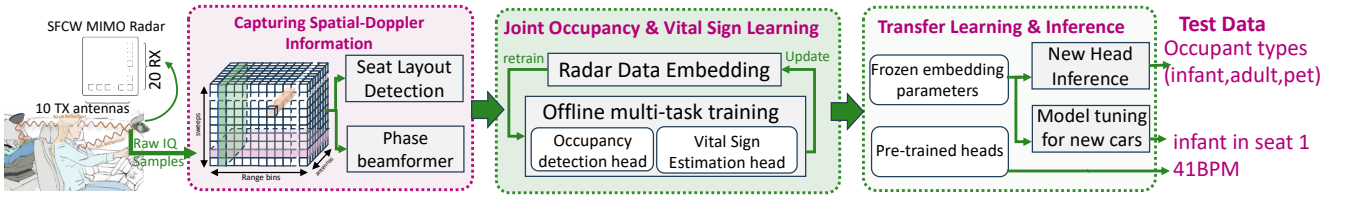

Figure 3: System overview

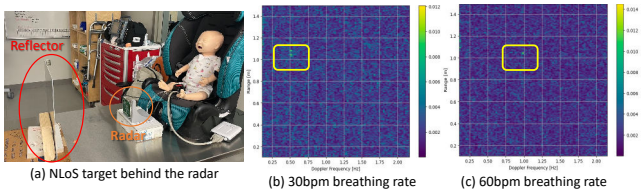

(a) NLoS target behind the radar (b) 30bpm breathing rate (c) 60bpm breathing rate

Figure 4: Feasibility of detecting the infant's vital signs through multipath reflections off of a metal reflector.

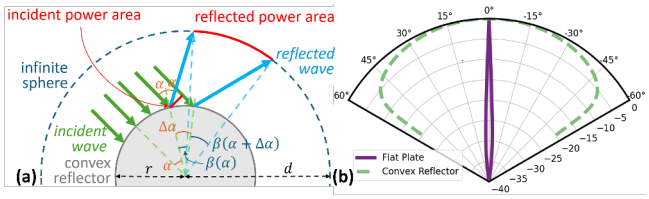

Figure 5: (a) Geometric model of convex reflector; (b) approximate normalized radiation pattern (dB) of plate and convex reflectors for incident angle = 0° waves.

infant wellness monitoring. BSENSE consists of four main modules: (1) synthetic passive reflectors that seamlessly work with the radar to cover blindspots and NLoS areas (2) a Spatial-aware digital beamforming pipeline for extracting micro-Doppler and phase information of different zones in the car while boosting the SNR, (3) a joint occupancy and vital sign learning framework that transforms the complex LoS and NLoS reflections into location and respiration rate related information, (4) a transfer learning technique for automatically learning the seat layouts of a new car and adapting to new vehicles. This section describes each of these components in detail.

3.1 Synthetic Reflectors for NLoS Coverage

BSENSE places a mmWave radar under the rear mirror in front of the car and synthetic reflectors on the corners of the car in the back rows to cover NLoS areas. These reflectors can be easily fabricated into the car frames with negligible extra cost. To demonstrate the effectiveness of this solution, a controlled experiment is performed in Figure 4 by placing a metal reflector in front of an infant simulator and the radar facing the reflector but not the infant simulator. From the range-Doppler profile, we can see the infant's respiration signal through the metal reflector. However, detection the second-order reflections from human body off of random surfaces in the car may not work well for different child sizes, positions, and orientations. To address this, we propose the design of a custom synthetic reflector with certain shape and size using the laws of RF reflection from a convex surface [68].

Shape of BSENSE Synthetic Reflector: Passive RF reflectors of different shapes are used in previous works for varying applications, such as parabolic reflectors at the backside of the antennas to focus the energy beam in a given direction [74], or large flat metallic reflectors for point-to-point base station communications [48]. However, the purpose of using synthetic reflectors in this project is to diverge the incoming rays in multiple directions, thus increasing the field of view of the radar in blind spots. To achieve that, we utilize convexly curved metal reflectors in the form of half spheres, which demonstrate a greater azimuth and elevation angular scattered field relative to a flat surface [34, 79]. To provide an approximate model of the reflected signal power from a convex reflector with radius r, consider the reflected signal reaching an infinitely far sphere with radius $d \gg r$. We denote a specific ray's angle of incidence as α. As shown in Figure 5(a), two adjacent rays with central angles α and $\alpha + \Delta\alpha$ has incident power proportional to the area transverse to the propagation direction, *i.e.* $P_{\text{inc}} \propto \sin(\alpha + \Delta\alpha) - \sin\alpha$. We further define the central angle $\beta(\alpha)$ between the incidence point and reflected ray's intersection with the far-field sphere as a function of α. $\beta(\alpha)$ can be implicitly derived by the law of Sinusoid as

$$\frac{\sin(\alpha)}{d} = \frac{\sin(\alpha - \beta(\alpha))}{r} \tag{3}$$

The incident power P_{inc} is then being reflected to an angle of $\Delta\alpha + \beta(\alpha + \Delta\alpha) - \beta(\alpha)$ at the infinite sphere. Thus, the far-field bi-static radiation pattern G can approached as

$$G(\alpha + \beta(\alpha)) \propto \lim_{\Delta\alpha \to 0} \frac{\sin(\alpha + \Delta\alpha) - \sin\alpha}{\Delta\alpha + \beta(\alpha + \Delta\alpha) - \beta(\alpha)} \tag{4}$$

Leveraging this equation, we compare the theoretical radiation pattern of a convex reflector along with a flat-plate reflector in Figure 5(b). Spherical reflectors redirect the EM-waves toward a large angular area instead of to a specific direction, allowing better coverage of the infant's potential locations. In addition, the spherical reflectors can preserve this wide reflection pattern regardless of the incident angle. It should be noted the size of the reflector does not change the radiation pattern (*i.e.* G is independent of r). However, the reflector size affects the total power received from the radar and reflected toward new directions. As such, the reflector size can be carefully selected based on the radar's transmit power to achieve blind spot coverage but avoid excessive interference.

Reflector Placement: To effectively capture the second-order reflections from rear-faced infants, the synthetic reflectors should be placed in the LoS of the radar. In addition, to avoid ambiguity in different seat occupancies, we expect both LoS and NLoS reflections

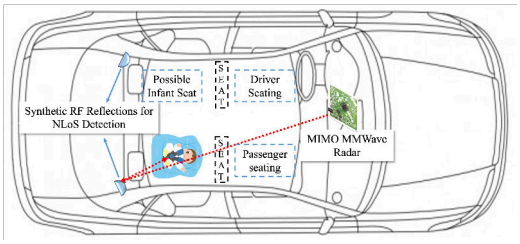

Figure 6: Reflector arrangements for covering NLoS.

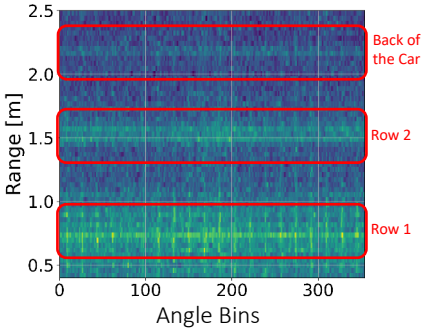

Figure 7: Radar reflections for each seat row in the car appear across different angles within a range bin.

for each seat to fall in the same angular area in radar images. As such, we use two reflectors at the two upper back corners of the car interior, as shown in Figure 6, where each reflector can capture the NLoS occupancy of their corresponding seat while preserving the angle of reflections.

3.2 Capturing Spatial-Doppler Information

The goal of BSENSE's first processing component is to transform raw radar data into spatial and spectral features reflecting from each voxel in the 3D space. This allows us to estimate both seat occupancy and vital signs, to then estimate child presence based on standard respiration rates across ages [76]. A simple approach for extracting this information is to use FFT and identify the peak Doppler frequency corresponding to the breathing rates at any given ⟨range, elevation, azimuth⟩ voxel. However, the small Radar-Cross-Section of the infant's body only creates a very weak reflection that can be easily masked by more dominant movements in the environment, even after background subtraction. Beamforming is an alternative approach for boosting SNR of these reflections by focusing on the direction of reflections coming from people in the car. However, we do not know the exact location or orientation of the occupants in the car, or their respiration rates, which creates a very large beamforming search space. To address this trade-off, BSENSE combines FFT and phase beamforming to focus on areas with the maximum likelihood of reflections from the occupants' bodies. Specifically, it decomposes into three main processing chains: (1) Finding car seat layout as a coarse localization to reduce the search space, (2) capturing condensed spectral features using 4D FFT within the areas of interest, (3) boosting SNR and capturing micro-Dopplers in the time-space domain through phase beamforming.

Car Interior Layout Detection: During sensor deployment, BSENSE finds the vehicle's interior configuration by identifying the car seat rows. This not only provides insights into the positioning of front-facing and rear-facing car seats but also enables our infant detection algorithm to adapt dynamically to different car sizes and models. The underlying intuition is that the radar reflections from each seat row appear consistently across all angles at a fixed distance. To identify the seat reflections, BSENSE first finds the radar range profile. We use a MIMO SFCW radar with 10 transmitting antennas on the elevation plane and 20 receiving antennas on the azimuth plane. Therefore, each received radar frame is a 3-D matrix of $[10, 20, 150]$ size, which contains the amplitude and phase changes of 150 frequency steps across the radar bandwidth. The phase difference of received signals across different frequency steps is a function of objects distance to the radar. It can be estimated by a simple Inverse Fast Fourier Transform (IFFT) on frequency sweeps. To extract the high-resolution angular pattern, BSENSE next leverages 2D digital beamforming per range bin across transmitting and receiving antennas. The resulting range-angle profile can then be used to find the seat layouts in the car, as shown in Figure 7. It should be noted that car layout detection is a one-time task during the sensor deployment, so the computational cost of high-resolution beamforming can be neglected.

4D Spatio-Spectral Imaging: After finding the seat layouts in the car, BSENSE extracts the range bins before each seat row for occupancy and vital sign detection. It should be noted that the NLoS reflections from rear-facing car seats in the backseat row appear in the range bins after row 2 due to the longer travel time of reflections from radar to the synthetic reflectors to the infant's chest. As such, for a 2-row car, 3 range-bin groups should be extracted. Next, BSENSE extracts the spatio-spectral information for each range-bin group corresponding to each seat row based on the steps shown in Figure 8. After extracting the range profile (step 1), BSENSE performs a 2D angle-FFT across transmitting and receiving antennas per range bin (steps 2 and 3) and a Doppler-FFT across frames within a time window (steps 4 and 5). This results in Range-Doppler profiles per Azimuth-Elevation angles, representing prominent frequency components in the 3D space, potentially from adults or major movements in the car.

Temporal Locality Capture Through Beamforming: While the extracted FFT-based Doppler profile contains coarse spectral information across the 3D space, it may still miss the weak reflections with breathing information of infants or the spectral information for varying breathing rates. To address this issue, BSENSE leverages phase beamforming principles [38] across the azimuth and elevation angles of each range-bin group. Using phase-beamforming not only provides SNR improvement but also captures the temporal locality of vital signs for each row. To reduce the search space, we segment the azimuth plane into 10-degree cells to distinguish between seats and the elevation plan into 10-degree cells to capture car occupants with different heights. Finally, BSENSE coherently combines the phases of beamformed signals across different range bins of each row by using the delay-and-sum method [70]. The final output of the beamformer is a 3D cube with azimuth-elevation-phase information across frames, which is then sent to the joint occupancy and vital sign detection module along with the 4D Spatial-spectral images of the previous step.

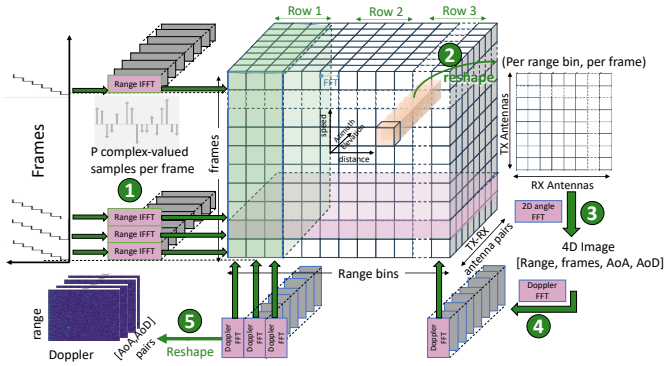

Figure 8: BSENSE converts the raw radar data into a 4D micro-Doppler images to extract spatial-Doppler information.

Note that combining FFT and beamforming outputs provides us with spatial features of both spectral and temporal patterns. This combination is particularly effective as one focuses on emphasizing adult reflections, while the other brings out weaker reflections from infants. Furthermore, while phase-beamforming is adept at detecting vital signs when the subject is static, incorporating Doppler information across range bins enables the model to differentiate movement information from other body parts, such as arms and head. Consequently, the integration of both sets of features results in a comprehensive feature representation that enhances the overall system's performance.

It is also worth noting that the two 2D beamforming performed for car layout detection and phase extraction are algorithmically the same but performed with different search space sizes, one including all range bins and magnitude values (for layout detection) vs. the other only applying to per row range-bin group representing each seat zone and phase values. In addition, to improve the SNR of chest reflections further, phase-beamforming is done after background subtraction and the removal of static reflections, while seat layout detection is performed without background subtraction.

3.3 Joint Occupancy & Vital Sign Learning

The goal of this component is to translate the spectral and spatiotemporal features into seat occupancy and their corresponding breathing rates. This is achieved without making any assumptions about the position of occupants, their respiration rate, or the number of people in the car. We demonstrate that while traditional seat occupancy or vital sign detection algorithms are not individually effective without making any of these assumptions, the joint learning and inference of occupancy and vital signs can use each model to define a constrain on estimation of the other model.To achieve this, BSENSE first transforms high dimensional spectral and spatiotemporal images for each car row to occupancy and vital sign embedding and then performs multi-task learning by adding downstream prediction heads for occupancy and vital sign estimation. The estimation results of each head could jointly learn and update the occupancy and vital sign radar representation embedding. We elaborate on each of these components next.

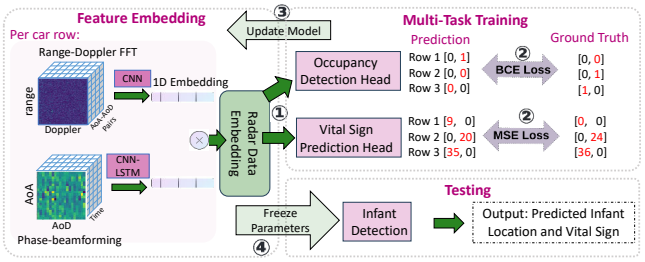

Figure 9: BSENSE jointly learns the location and vital sign features by using an embedding function and multi-task heads.

Feature Embedding: The pre-processing component explained in the previous section creates two sets of features for each time window per range-bin group (each representing a seat row): (1) 3D ⟨range-doppler-angle⟩ profile that represents the spatio-spectral features (2) and 3D beamformed ⟨azimuth-elevation-phase⟩ profile that represents the spatio-temporal features. BSENSE combines this information through a feature extraction embedding function using CNN and CNN-LSTM models, respectively, as shown in Figure 9. Each of these models results in a 1D embedding, which are then concatenated using a weighted sum attention module. The final representation embedding contains occupancy and vital sign information for each car row.

Multi-task Learning: The embedding vector for each row is then sent to a multi-task learning module [61] that consists of two multi-layer perceptron (MLP) prediction heads: (1) occupancy predictor and (2) breathing rate predictor. As shown in Figure 9, each head outputs occupancy or breathing rate per seat. Using ground truth data of occupied seats and the corresponding vital signs per row, the heads collaboratively update the representation model through gradient decent to enhance feature extractions for both location and respiration. Note that BSENSE learns head models in parallel per row. This enables tuning the parameters based on the reflection power which is proportional to their distance from the radar.

The occupancy detection head is a multi-label classifier that uses Binary Cross Entropy between the target and prediction in the loss function. The vital sign prediction head is a regression model that uses the Mean Squared Error (MSE) of the predicted and estimated respiration rate in breaths-per-minute (BPM) across the two seats in each row.

3.4 Transfer-learning for New Cars

Given the generic feature embedding used in the radar data pre-processing, the inferences based on multi-task learning are expected to perform well in the same environment across different users or different cars of the same size and layout. However, the performance may drop in a new car with a different seat arrangement. Inspired by the recent transfer learning approaches [23], BSENSE uses a domain adaptation framework that utilizes the embedding parameters learned in one car and fine-tunes the multi-task prediction models by just using a small amount of annotated data in the new car at the time of radar deployment. This prevents over-fitting to the new small dataset and makes use of the pre-trained feature sets.

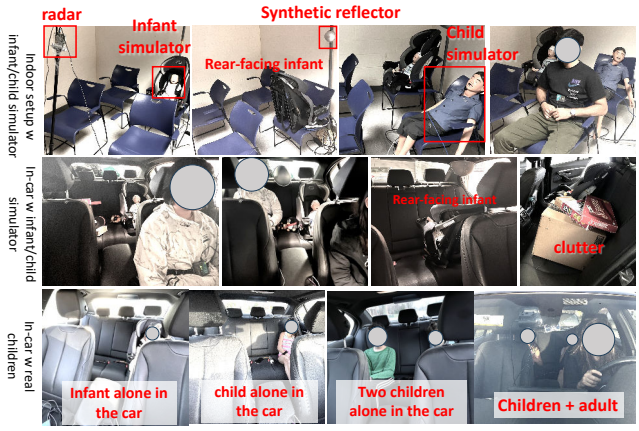

Figure 10: Indoor and in-car experimental setup with pediatric simulators and real children.

This framework can also be used to train a new task to offer more applications, such as occupant counting or classification. In this case, the output of pre-trained feature embedding will be passed to a new MLP head with appropriate loss function definition, such as Binary Cross-Entropy (BCE) for classification tasks and Mean Squared Error (MSE) for regression tasks. For example, to perform a classification task distinguishing between adults, children, and pets, we could add a new prediction head attached to the Radar Data Embedding and use Binary Cross-Entropy (BCE) loss for multi-class classification.

4 Implementation

Hardware: We implement BSENSE using the IMAGEVK-74 [1] Radar, a compact evaluation kit developed by Vayyar. It is equipped with 20×20 onboard transmitting and receiving antennas, emitting stepped-frequency continuous waveform (SFCW) within 62-69 GHz band. In order to maintain high temporal resolution for respiration recordings, we only use a 4 GHz bandwidth from 62-66 GHz, 10 Tx, and 20 Rx with 150 frequency steps and 50 kHz RBW. The radar connects to a host PC through a USB cable for data acquisition. We use aluminum hemisphere surfaces at each corner of the backseat row for synthetic reflectors. For infant and child simulators, we used SimBaby [5] and SimJunior [6] pediatric simulators, representing a 9-month and 6-year-old child, respectively. The simulators are highly realistic manikins that have a wide range of programmable respiration rates and movements. We use a Lambda machine with an A6000 GPU to pre-train the deep learning framework and an ASUS A15 gaming laptop for inference.

In our current implementation, we use a radar development kit ($3000) and a gaming laptop for inference ($1100). However, the final product can be made cost-effective by utilizing integrated radar chips and the Electronic Control Unit (ECU) already installed in modern vehicles for data processing; this is evidenced by similar integrated modules that cost less than $20 [12]. Additionally, the same radar can be used for multiple in-cabin applications beyond child detection, including driver monitoring, seat occupancy detection, passenger health monitoring, and gesture control for infotainment systems, making it more versatile than cheaper sensing modalities like acoustic sensors. This is further supported by recent announcements from major automotive companies adopting Vayyar radar for in-cabin sensing [11].

Software: We implement data collection, signal processing, and the proposed learning framework using Python 3.10. The architecture and training of the deep learning model is based on PyTorch 2.1.1. For the model with CNN backbone, we utilize the ResNet18 [40] with the number of CNN blocks equal to 3, kernel size to 3, and the number of channels to 16. For all prediction heads, we set the MLP head layers to 4. All the encoder weights θ_{encoder} (including backbone CNN and CNN-LSTM model), and prediction decoder weights θ_{decoder} follow random initialization.

4D FFT and Beamforming Pre-processing: for initial data processing, we perform a 512-bin range IFFT, offering a range resolution of 0.03m and a 2D angular beamforming of 20×20 grid, representing the (x, y) 2D space. For 4D spectral imaging, we use a 4×4 bin for angle FFTs and 128-bin for Doppler FFT, creating a 3D matrix of [4, 4, 128] per radar frame.

4.1 Experimental Setup

Data Collection: Our experiments, approved by our university's IRB, were carried out in two different environments: (1) indoor experiments that are performed in a controlled 4-seat setup that mimics the layout of a car, (2) car setups in three different car models (i.e., compact and full-size sedans and an SUV). Note that we excluded the middle backseat from our evaluations to better manage the number of experimental scenarios. Moreover, the open space between the radar and the middle backseat positions this seat within the line-of-sight (LoS) setting; thus, omitting this seat should not negatively impact the model's performance, as it typically presents clearer and less challenging conditions for detection. More than 400 unique experiments are performed, consisting of a mix of different numbers of infants or children in different seats (infants could be in front-facing or rear-facing car seat positions), either alone or accompanied by 1 to 4 adults at different seats. Overall, 10 adults and 5 children in healthy condition were recruited for this data collection in addition to two medical-grade simulators. No sensitive data like personal identifiers were collected. For experiments with the infant simulator, the data is collected for a range of respiration rates from 30-60 breaths-per-minute (BPM) for two orientations (front-facing and rear-facing). The experiments with the child simulator include a range of respiration rates from 20-40 BPM. During data collection, both simulators are set to mimic the casual body movements of real children, which will be more challenging and more realistic for respiration monitoring. Snapshots of our experimental setup are shown in Fig. 10. Each experimental scenario is conducted for 30 seconds and performed twice with different adults for generalization. The overall collected data results in 120,000 radar data points. For feature extractions, a 200-frame sliding time window (approximately 12s) is defined with 10-frame increments, resulting in an estimate of every 0.5s. The ground truth respiration rate of adults and real children is measured by NeuLog respiration monitor devices [3].

Training and Testing: To prevent overfitting and guarantee sufficient training data, we partition the collected data into training, validation, and testing datasets using the leave-one-experiment-out

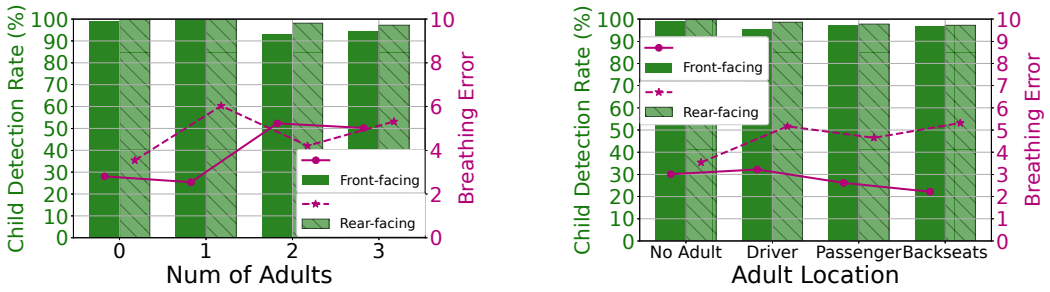

(a) Impact of # Adults **(b) Impact of Adult Location**

Figure 11: In-car child detection performance using a programmable infant simulator.

method and perform cross-validation over all the unique experiments. Multiple parameters could change across experiments, such as the number of occupants, the individual occupants, infant and children positions, their respiration rates (specifically for infant and child simulator), occupied seats, or the environment. As such, the trained model has not seen any test data with the exact same experimental setup, which avoids any correlation between the train and test set. We also demonstrate the generalizability capabilities of BSENSE by directly applying a pre-trained model on a different test person (Section 5.5) or a new environment with a small set of augmented data (Section 5.2).

Baselines: We compare BSENSE to baseline implementations of respiration estimation that perform standard beamforming and Doppler-FFT processing with the same data preprocessing steps in section 5.5. The baseline algorithm executes beamforming and Doppler-FFT across all frames in an experiment. It then identifies the peak frequency within the specified peak range, as determined by beamforming, to estimate the BPM. It should be noted that we exclude baselines based on other sensing modalities or UWB radars due to their far less spatial and range resolution, resulting in an unfair comparison. In addition, we exclude existing deep learning-based CPD methods due to their inability to perform multiple people joint infant and respiration detection and their dependencies on certain types of training data with hyperparameter ambiguities. We will also perform an ablation study to show the importance of each component in BSENSE performance.

Evaluation Metrics: The presented occupancy detection results are F1 scores across different seats, and the child detection rate is the percentage of accuracy estimating the presence of a child at the correct seat across all test data. BPM Error is also presented as Mean Absolute Error (MAE).

5 Evaluation

5.1 In-car Performance w/ Child Simulators

We conducted a comprehensive study in real cars with 10 different adults and an infant simulator with programmable respiration rate. The overall performance of BSENSE across all these experiments is shown in Figures 11a and 11b. We can see that BSENSE can accurately detect the infant with or without the presence of adults in the car in both front-facing and rear-facing positions. In addition, the infant's breathing rate can be accurately estimated with less than 6 BPM error. Figure 11a also shows that the child detection accuracy drops slightly for larger number of adults in the car due to high signal variations. However, this lower performance is acceptable as infant's wellbeing risk is much lower in the presence of more adults in the car overseeing the infant. In cases where the child is alone, the system's accuracy remains high enough (around 99%) to prevent dangerous situations, such as unattended children in the car. Figure 11b also shows that BSENSE performance is not dependent on the location of people in the car.

It is worth noting that the slightly higher performance of BSENSE for rear-facing children in backseat scenarios is due to radar's placement at the rearview mirror. This positioning can sometimes cause the front seat to obstruct the view of a child or infant in the backseat in certain line-of-sight (LoS) scenarios. The RF reflector is specifically designed to enhance non-line-of-sight (NLoS) monitoring performance. Thus, the system generally performs slightly better in rear-facing cases compared to front-facing cases, but the difference is negligible.

5.2 In-car Performance w/ Real Children

Next, we test BSENSE performance in real-world setups involving human infants, young children, and adults across various car models and parking scenarios (e.g. indoor parking lot, roadside parking, and garage). The data is collected across multiple days and participants had different type of clothing including winter coats. Normal vehicular and pedestrian traffic existed around the experimental vehicle during data collection. Five different age groups of children (ranging from 10 months to 10 years old, 2 girls and 3 boys) and five different adults participated in these experiments, across three types of vehicles: a compact sedan, a full-size sedan, and a mid-size SUV.

Overall Performance: Figure 12a illustrates the average child detection rate (their presence and correct location) of 98.6% across different children of different age and size. There is a minor performance reduction for child4, which is a 10 year old boy with larger than average body size for their age. This confirms the potential challenges of distinguishing a subset of children with overlapping body size and breathing rate compared to adults. However, BSENSE can maintain the high performance for infants with higher threats if left unattended in the car.

Unattended Child Detection Accuracy: Next, we show BSENSE performance in differentiating between an unattended child and clutter in the car or when adults are present. Figure 12b compares

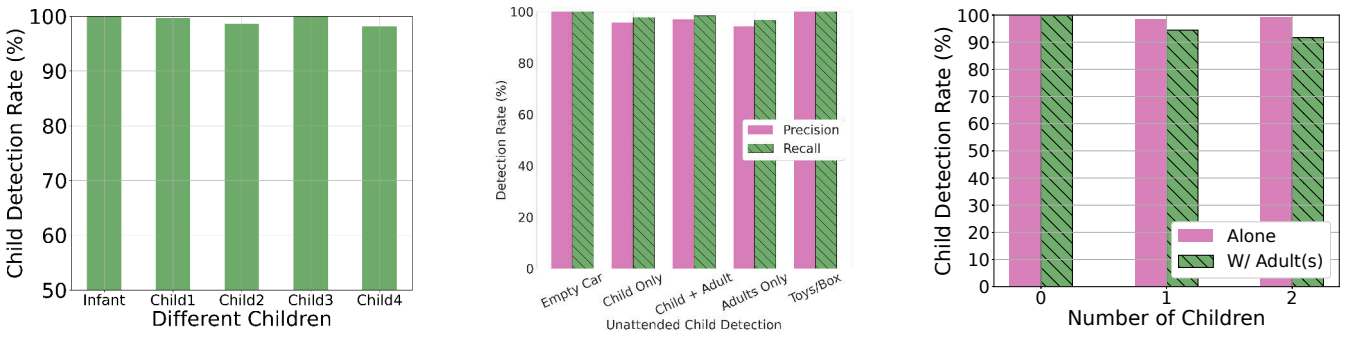

(a) Overall Performance (b) Unattended Child Detection (CPD) (c) Impact of Number of Children

Figure 12: BSENSE real-world performance for 5 different children ranging from 10 months to 10 years old.

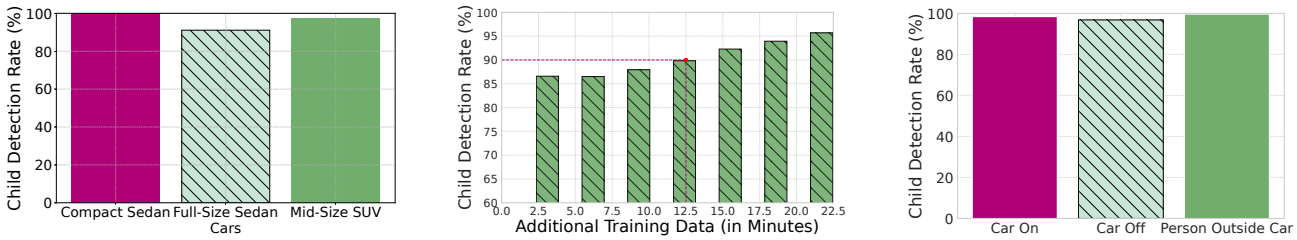

(a) Across Car Models (b) Data Augmentation in New Cars (c) Impact of Environment Interference

Figure 13: BSENSE generalizability across different car models and car states, while only requires 20 minutes of data augmentation to achieve above 95% accuracy in a new car.

the unattended child detection accuracy across different scenarios, such as empty car, presence of only children, children with adults, adult only, or clutter in the car. The performance remains consistently high, achieving over 95% accuracy across all tested scenarios. It should be noted that the children-only experiments include 1 or 2 kids in the car and the model is capable of correctly detecting those cases as unattended child situation. In addition, the "Adults only" condition in the unattended child detection tests serves as a crucial measure of our model's ability to effectively differentiate between adults and children. Meanwhile, all other conditions are used to assess the False Alarm Rate (FAR) for unattended child detection tasks.

Impact of Number of Children: Figure 12c elaborates on BSENSE performance for different number of children in the car, with and without the presence of adults. It is important to note that a reliable CPD system should be able to detect unattended children no matter how many infants or children are in the car. We can see that while children alone remains consistently accurate over different numbers of children scenarios, the performance slightly drops in the presence of 3 or more people in the car, when 2 kids are accompanies with one or multiple adults. The error is mainly caused by confusing the location of the children in the car as our detection metric expects accurate children presence and positioning detection.

Impact of Car Models and States: Figure 13a demonstrates BSENSE performance across different car sizes and models. For this evaluation, BSENSE was only trained for compact sedan and transferred as is to the other two car models. This demonstrates the effectiveness of interior layout detection. The proposed transfer learning approach can be used to further improve the performance of a new car by gradually adding a small set of annotated data. As shown in Figure 13b, a 20 minutes of data augmentation would be sufficient to fully personalize a pre-trained model in a completely different environment to new car models and sizes. Figure 13c also shows the impact of different car states (being on vs. off vs. people moving around outside the car) with minimal impact on child detection performance. This is mainly because the model learns the spatial distribution pattern of children or adults and can ignore other environmental changes.

5.3 Indoor Sensitivity Analysis

Using the infant and child simulators, we performed a comprehensive evaluation in indoor environments by programming the simulators for different breathing rates and collected data with varying number of infant, child, or adults in a 4-seat car model. The presented results show the testing accuracy using leave-one-experiment-out with cross validation across all unique experiments.

Robustness to Different Breathing Rate: We show BSENSE performance in detecting different infant or child breathing rates, either in front-facing or rear-facing positions. Figure 14a confirms BSENSE consistent performance in detecting child presence, location, and respiration rate across different scenarios. It should be noted that the overall detection rate is higher than the in-car experiments due to less occlusion and multipath condition of indoor space vs. car interior.

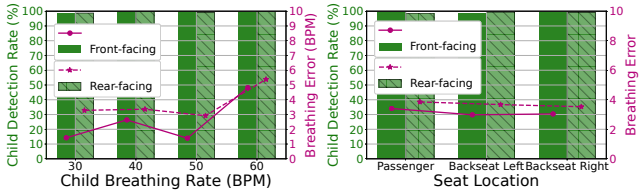

(a) Cross-BPM (b) Cross-infant Location

Figure 14: Sensitivity analysis of BSENSE for varying breathing rates, car seat orientation and positions.

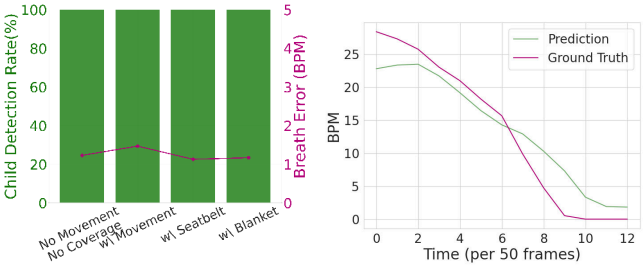

(a) Impact of Interference (b) Vital Sign Tracking

Figure 15: BSENSE is robust to (a) different environmental interference and (b) can accurately track the vital sign over time.

Robustness to Different Infant Positions: Figure 14b also shows BSENSE performance across different infant or child positions, and we can see that our child detection accuracy is robust in both row 1 (front row seats) and row 2 (back row seats) in the car as well as rear-facing conditions for infants.

Impact of Occlusion and Infant Movement: Compared to older children and adults, detecting infants are often more challenging due to their unpredictable movements and weaker vital signs. To evaluate the effectiveness of BSENSE across different potential interferences, we test common occlusions such as blankets and seatbelts or child movement. It should be noted that the infant simulator is capable of mimicking crying with similar body movements to a real infant. As demonstrated in Figure 15a, our method consistently performs well, maintaining stability in both child detection rate and breathing estimation despite movements and occlusions.

Vital Sign Tracking Over Time: Given the leveraged sliding time window, BSENSE is also capable of tracking the infant's respiration rate over time after detecting and positioning the infant. Figure 15b mimics a scenario where the respiration rate of the infant simulator is slowly dropping from 30 to 0 BPM and we can see that the predicted BPM value follows the ground-truth.

Average Detection Rate	No reflector	With Reflector of Size		
		Small	Medium	Large
	52.56%	88.89%	100%	100%
		96.30%		

Table 1: Detection rate with or without reflector.

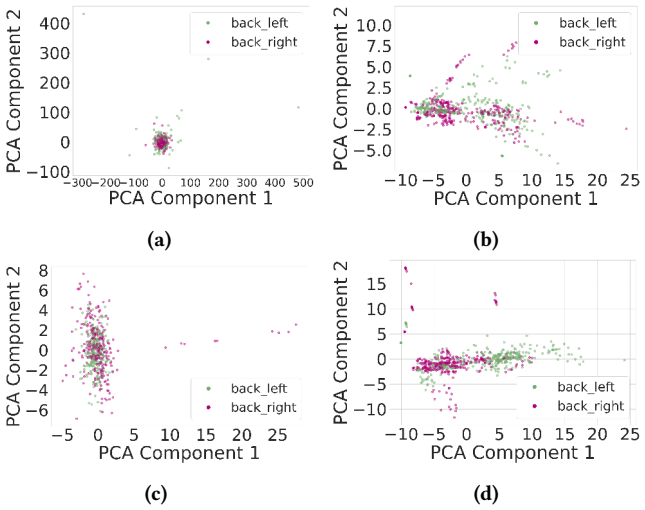

(a) (b) (c) (d)

Figure 16: PCA visualization of (a) pre-processed radar data; (b) Doppler-only embeddings; (c) phase-only embeddings; and (d) combined learned embeddings.

Impact of Synthetic Reflectors: To demonstrate the efficacy of synthetic reflectors in detecting infants in rear-facing positions, we conducted benchmarks on a rear-faced infant simulator seating in the backseat, with either no reflector or placing a reflector of different sizes (1.4, 2.5, 4 inch radius) in the corner of the car model. As shown in Table 1, the synthetic reflector is effective in improving child detection rate in NLoS scenarios, increasing the performance from 52% to an average of 96.30% across different reflector sizes.

5.4 Model Interpretation

To gain more insight into the efficacy of BSENSE learned embedding, we visualize the two principal components of the learned embedding vs. pre-processed data before embedding in Figure 16. As we can observe, the preprocessed features generated by signal processing methods (beamforming and FFT) can hardly distinguish the representation of left and right backseats. Whereas, BSENSE can achieve significantly better seat separation after embedding (Figure 16d). In addition, we can see the importance of combining phase and Doppler information to distinguish different seat occupancy and breathing rates.

5.5 Ablation and Benchmark Study

Model Ablation: To investigate the effectiveness of our proposed joint occupancy detection and vital sign estimation approach, we perform an ablation study using only one prediction head to estimate either occupancy or vital sign. Table 2 shows the effectiveness

	Joint occupancy and Vital sign prediction		Only occupancy/ Vital sign prediction	
	infant only	infant+adult	infant only	infant+adult
Vital sign prediction	2.48	3.54	6.49	6.53
Occupancy detection	99.67%	98.69%	97.81%	95.37%

Table 2: Ablation study results showing the effectiveness of joint occupancy and vital sign learning.

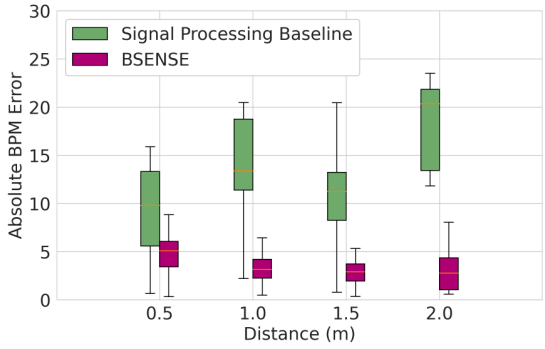

(a)

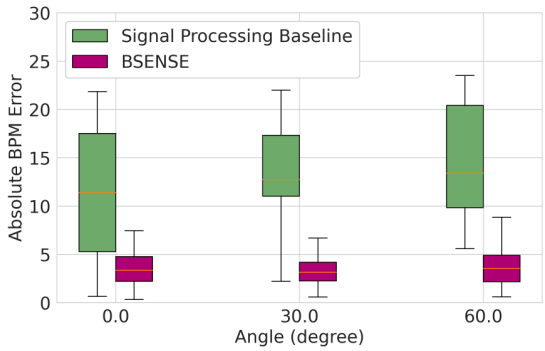

(b)

Figure 17: Benchmarking BSENSE vital sign detection across (a) different distances and (b) orientations, compared to existing signal-processing methods.

of multi-task joint learning. Given that any failure to detect the presence of a child could potentially result in life-threatening consequences, even a 3% reduction in detection accuracy is significant and can substantially increase the risk of dangerous outcomes.

Impact of Distance and Orientation: We also conducted indoor benchmarking tests with adult subjects in three different environments (apartment, laboratory, and classroom) at different distances (0.5-2.0 m) and orientation (0-60 degrees) from the radar and compared BSENSE performance with signal processing baselines using leave-on-subject-out testing. As shown in Figure 17, BSENSE consistently outperformed the baseline methods across all tested distances and orientations. BSENSE consistently maintains a low respiration error rate for each adult, with an average error below 5 BPM. In addition, the leave-one-subject-out testing used in these benchmarks demonstrates BSENSE generalizability without overfitting. This is notable because no data augmentation for tuning to new environments or subjects is used in these benchmarks.

6 Related Work

In-car sensing solutions for driver or child monitoring have seen great developments in the past few years. These methods can be classified into two broad categories — contact-based and contactless solutions.

Contact-based In-car Sensing: The most common contact-based seat occupancy detection in cars make use of pressure [33], temperature [17], or capacitive [26, 35] sensors embedded in car seats. However, false alarm rate is the major issue as these methods are heavily dependent on the position of the child and the sensor [33, 49]. Furthermore, all these approaches lack vital sign detection to differentiate an object from a human.

Contactless In-car Sensing: Recent methods take advantage of remote sensing techniques such as PIR sensors [55, 83], cameras [21, 67], acoustic [22, 37, 72, 87, 107], WiFi [46, 71, 103], and radars [66, 97]. These methods mainly rely on detecting motions in the car and correlating them with human movements or body movements due to breathing. However, each of these approaches presents its own set of limitations. Both PIR sensors and cameras are sensitive to environmental changes, including variations in temperature or lighting conditions [67, 77]. Cameras can introduce privacy issues, but also suffer from non-line-of-sight limitation, especially in rear-facing car seats.

WiFi In-car Sensing: WiFi-based in-car sensing systems rely on motion detection either by monitoring temporal changes or in reference to a channel measurement when the car is empty [46, 71, 102, 103]. A few works have also focused on respiration detections with WiFi, but they are limited to LoS [104, 105]. The fundamental challenge in using WiFi for in-car sensing is the resolution limitation [42] due to small available bandwidths, small number of antennas, and sampling and carrier frequency offsets, which make it hard to detect and monitor the vital signs of little infants.

Acoustic In-car Sensing: This group of papers either leverage environmental sound or active acoustic sensors for human presence detection or vital sign monitoring using the speaker and microphone system available on devices [37, 63, 72, 82, 87, 88]. Similar to radio-based solutions, these systems leverage phase changes, Time of Flight, Doppler shift, or statistical features to correlate the temporal changes with human movements. However, acoustic sensing typically suffers from serious multi-path problems due to the nature of sound waves. A recent study, VeCare[107], made use of the existing speaker-microphone inside the car, tried to address multipath challenge by deriving motion statistics from all reflected paths. However, this technique still faces difficulties in distinguishing between multiple passengers. The fundamental challenge is that combining all the signals to infer movement and respiration patterns will inevitably confound the individual signatures of each occupant. In addition, the limited spatial resolution of commodity microphone sensors does not allow accurate separation of multipath signals from different people in the car.

Radar In-car Sensing: Radar-based solutions [14, 32, 44, 50, 51, 56, 57, 84, 93] have shown much more promise for human sensing than the other described methods. Even though they require an additional attachment, they can be used universally and have a comparatively higher accuracy rate for vital sign monitoring. As a result, many car manufacturers like Toyota and Volvo are moving towards radar solutions for child presence detection [7, 11]. The most commonly used radars are the IR-UWB [31, 50, 54, 56, 65, 73, 94, 99, 100] and FMCW radars [14, 57, 59, 69, 81, 84, 90, 95, 96]. The IR-UWB radar is a pulsed radar that can provide highly accurate vital sign measurements but it lacks spatial resolution as these radars typically come with a single transmitting and receiving antennas.

Table 3: Comparison of various In-Car Sensing Solutions for Child Monitoring

Methods	Sensing Modality	Application	Coverage	Single-Point Sensing	Multi-Person Scenarios	Infant Detection
VeCARE [107]	Acoustic	Unattended Child Detection	LoS/NLoS	✗	✗	✓
Distributed Acoustic [82]	Acoustic	Unattended Child Detection	LoS/NLoS	✗	✗	✓
WiCPD [103]	WiFi	Unattended Child Detection	LoS/NLoS	✗	✗	✓
CarOSense [65]	UWB Radar	Car Occupancy Detection	LoS only	✓	✓	✗
Vital-Radio [18]	FMCW Radar	Vital Sign Monitoring	LoS only	✓	✗	✗
BSENSE	SFCW mmWave Radar	Child Detection & Monitoring	**LoS/NLoS**	✓	✓	✓

Millimeter-wave radars, on the other hand, offer high spatial resolution thanks to their millimeter-level wavelength and small antenna form factor. However, the existing in-car mmWave sensing solutions either focus on adult passenger monitoring [24, 57, 91], or LoS cases [14], lacking detection in NLoS scenarios and blind spots. Our proposed method addresses these limitations by jointly estimating location and vital signs, which allows us to accurately detect the weak reflections from an infant's body even in the presence of other dominating reflections, such as those from an adult. In addition, we proposed a synthetic reflector setup to cover NLoS areas while preserving the single-point sensing feature of radars.

mmWave-based Human Sensing: mmWave sensing has been an active area of research in recent years, and various applications have been studied, including pose estimation [66, 97], temperature monitoring [27], object or material recognition [39, 78], imaging [20], spatial estimation [43], simultaneous mapping and localization [25, 53, 98], and vital sign monitoring [18, 29, 36, 45, 62, 75, 101]. These works either explore super-resolution signal processing techniques or end-to-end Deep learning on top of radar heatmaps. However, neither of these works is directly applicable to in-car sensing due to high multipath and NLoS conditions inside the car. In addition, the previous vital sign monitoring solutions make assumptions either on the known location and orientation of the users or known respiration rates of adults, neither of which would be held in the car scenario, especially for infant wellness monitoring. We have summarized the comparison of various latest in-car sensing solutions for child monitoring in Table 3.

7 Discussion

BSENSE achieves child detection, localization, and vital sign monitoring using a single mmWave radar without making any assumptions about the presence of adults or child orientation and position in the car. Nevertheless, BSENSE still has some limitations, and there are few unaddressed avenues for future improvements:

Experimental Extension: To demonstrate the effectiveness of BSENSE in detecting and monitoring child presence, the system has been tested on healthy subjects and child simulators during short experimental windows, adhering to our IRB protocol. However, the realism and robustness of BSENSE could be further tested and enhanced through three proposed future experiments: (i) Expanding the dataset to include more vital sign data from real infants, rather than relying solely on SimBaby and SimJunior simulators. (ii) Conducting long-term reliability and consistency longitudinal studies, allowing us to observe any variability in the system's functionality. (iii) Expansion to more car models. Testing BSENSE in a wider variety of car models, including 3-row vehicles.

BPM Estimation Performance: An average BPM error of up to 6 BPM is considered relatively high in healthcare applications where precision is critical. However, This lower accuracy does not affect BSENS performance as it mainly uses vital sign for differentiating adults from children or monitor dangerous variations.

BSENSE Effective Areas: Our current child detection algorithm is tuned for the seating areas and ignores unconventional scenarios such as the presence of unattended children in leg areas. It would be more beneficial to extend functionality by placing more RF-reflectors in the proper location to detect unattended children in arbitrary locations within a vehicle.

8 Conclusion

To summarize, BSENSE combines signal processing and deep learning methods to robustly learn seat occupancy and vital sign information in the car and use it for detecting the presence of an infant or child in the car and monitoring their vital signs. BSENSE achieves this without making any assumptions about where and how the infant is seated in the car or the presence of adults. The evaluation results show promising performance in many real-world in-cabin scenarios, including both forward-facing and rear-facing positions, with and without adults.

Acknowledgments

We are grateful to Chaoyang Yin and Anushri Mittal who assisted in conducting the experiments and to our anonymous participants for their valuable contributions. We also extend our thanks to sim center at UIUC and Texas Instrument for their valuable hardware and technical feedback. This project was partially funded by NSF Award #2414227.

References

[1] 4D Millimeter Wave Radar Kit. https://www.minicircuits.com/WebStore/imagevk_74.html.

[2] Child passenger safety requirements. https://www.ilsos.gov/departments/drivers/childsafety.html.

[3] Neulog sensors. https://neulog.com/respiration-monitor-belt/.

[4] Push for imaging radar for in cabin sensing. https://www.automotiveworld.com/articles/4d-imaging-radar-could-solve-growing-complexity-of-in-cabin-safety/.

[5] Simbaby pediatric simulator. https://laerdal.com/us/products/simulation-training/obstetrics-pediatrics/simbaby/.

[6] Simjunior pediatric simulator. https://laerdal.com/us/products/simulation-training/obstetrics-pediatrics/simjunior//.

[7] World-first interior radar system from volvo cars helps you ensure that no one is left behind. https://www.media.volvocars.com/global/en-gb/media/pressreleases/304451/world-first-interior-radar-system-from-volvo-cars-helps-you-ensure-that-no-one-is-left-behind. Accessed: 2023-07-19.

[8] National highway traffic safety administration, heat stroke stats. https://www.nhtsa.gov/campaign/heatstroke, 2022.

[9] Vayyar child presence detection. https://vayyar.com/auto/solutions/in-cabin/cpd/, 2023.

[10] Car seat laws by state and country. https://saferide4kids.com/car-seat-laws-by-state/, 2024.

[11] How toyota connected 'cabin awareness' concept detects occupants. https://vayyar.com/blog/automotive/toyota-connected-cabin-awareness-concept-uses-new-tech-to-detect-occupants/, 2024.

[12] Single-chip 60-ghz to 64-ghz intelligent mmwave sensor integrating processing capability. https://www.ti.com/product/IWR6843/part-details/IWR6843ABGABL, 2024.

[13] H. Abedi, J. Boger, P. P. Morita, A. Wong, and G. Shaker. Hallway gait monitoring using novel radar signal processing and unsupervised learning. *IEEE Sensors Journal*, 22(15):15133–15145, 2022.

[14] H. Abedi, M. Ma, J. He, J. Yu, A. Ansariyan, and G. Shaker. Deep learning-based in-cabin monitoring and vehicle safety system using a 4d imaging radar sensor. *IEEE Sensors Journal*, 2023.

[15] H. Abedi, C. Magnier, V. Mazumdar, and G. Shaker. Improving passenger safety in cars using novel radar signal processing. *Engineering Reports*, 3(12):e12413, 2021.

[16] H. Abedi and B. Zakeri. Through-the-multilayered wall imaging using passive synthetic aperture radar. *IEEE Transactions on Geoscience and Remote Sensing*, 57(7):4181–4191, 2019.

[17] M. F. Abulkhair, A. Aldahiri, H. Alkhatabi, H. Alonezi, L. Mulla, and S. Razzaq. Sensor based hyperthermia alert car application. *Communications on Applied Electronics*, 5(2):44–55, 2016.

[18] F. Adib, H. Mao, Z. Kabelac, D. Katabi, and R. C. Miller. Smart homes that monitor breathing and heart rate. In *Proceedings of the 33rd annual ACM conference on human factors in computing systems*, pages 837–846, 2015.

[19] N. Administration. You can help prevent hot car deaths | nhtsa. https://www.nhtsa.gov/child-safety/you-can-help-prevent-hot-car-deaths, 2022.

[20] R. Appleby and R. N. Anderton. Millimeter-wave and submillimeter-wave imaging for security and surveillance. *Proceedings of the IEEE*, 95(8):1683–1690, 2007.

[21] C. K. O. Azaiz and J. D. Ndengue. In-cabin occupant monitoring system based on improved yolo, deep reinforcement learning, and multi-task cnn for autonomous driving. In *Fifteenth International Conference on Machine Vision (ICMV 2022)*, volume 12701, pages 295–304. SPIE, 2023.

[22] G. Beltrão, R. Stutz, F. Hornberger, W. A. Martins, D. Tatarinov, M. Alaee-Kerahroodi, U. Lindner, L. Stock, E. Kaiser, S. Goedicke-Fritz, et al. Contactless radar-based breathing monitoring of premature infants in the neonatal intensive care unit. *Scientific Reports*, 12(1):5150, 2022.

[23] Y. Bengio. Deep learning of representations for unsupervised and transfer learning. In *Proceedings of ICML workshop on unsupervised and transfer learning*, pages 17–36. JMLR Workshop and Conference Proceedings, 2012.

[24] S. Björklund, H. Petersson, A. Nezirovic, M. B. Guldogan, and F. Gustafsson. Millimeter-wave radar micro-doppler signatures of human motion. In *2011 12th International Radar Symposium (IRS)*, pages 167–174. IEEE, 2011.

[25] A. Blanco, P. J. Mateo, F. Gringoli, and J. Widmer. Augmenting mmwave localization accuracy through sub-6 ghz on off-the-shelf devices. In *Proceedings of the 20th Annual International Conference on Mobile Systems, Applications and Services*, pages 477–490, 2022.

[26] A. Braun, S. Frank, M. Majewski, and X. Wang. Capseat: Capacitive proximity sensing for automotive activity recognition. In *Proceedings of the 7th International Conference on Automotive User Interfaces and Interactive Vehicular Applications*, AutomotiveUI '15, page 225–232, New York, NY, USA, 2015. Association for Computing Machinery.

[27] B. Chen, H. Li, Z. Li, X. Chen, C. Xu, and W. Xu. Thermowave: a new paradigm of wireless passive temperature monitoring via mmwave sensing. In *Proceedings of the 26th Annual International Conference on Mobile Computing and Networking*, pages 1–14, 2020.

[28] R. Cheng, W. Heinzelman, M. Sturge-Apple, and Z. Ignjatovic. Deployment of a wireless ultrasonic sensor array for psychological monitoring. In *International Conference on Sensor Applications, Experimentation and Logistics*, pages 56–67. Springer, 2009.

[29] H.-R. Chuang, H.-C. Kuo, F.-L. Lin, T.-H. Huang, C.-S. Kuo, and Y.-W. Ou. 60-ghz millimeter-wave life detection system (mlds) for noncontact human vital-signal monitoring. *IEEE Sensors Journal*, 12(3):602–609, 2011.

[30] C. J. Cole. System to detect the presence of an unattended child in a vehicle, Jan. 30 2007. US Patent 7,170,401.

[31] X. Dang, J. Zhang, and Z. Hao. A non-contact detection method for multi-person vital signs based on ir-uwb radar. *Sensors*, 22(16):6116, 2022.

[32] A. R. Diewald, J. Landwehr, D. Tatarinov, P. D. M. Cola, C. Watgen, C. Mica, M. Lu-Dac, P. Larsen, O. Gomez, and T. Goniva. Rf-based child occupation detection in the vehicle interior. In *2016 17th international radar symposium (IRS)*, pages 1–4. IEEE, 2016.

[33] C. Fischer, B. Tibken, and T. Fischer. Left behind occupant recognition in parked cars based on acceleration and pressure information using k-nearest-neighbor classification. In *2010 IEEE intelligent vehicles symposium*, pages 1242–1247. IEEE, 2010.

[34] A. P. Ganesh, W. Khawaja, O. Ozdemir, İ. Güvenç, H. Nomoto, and Y. Ide. Propagation measurements and coverage analysis for mmwave and sub-thz frequency bands with transparent reflectors. In *2023 IEEE 97th Vehicular Technology Conference (VTC2023-Spring)*, pages 1–6. IEEE, 2023.

[35] B. George, H. Zangl, T. Bretterklieber, and G. Brasseur. A combined inductive–capacitive proximity sensor for seat occupancy detection. *IEEE Transactions on Instrumentation and Measurement*, 59(5):1463–1470, 2010.

[36] J. Gong, X. Zhang, K. Lin, J. Ren, Y. Zhang, and W. Qiu. Rf vital sign sensing under free body movement. *Proceedings of the ACM on Interactive, Mobile, Wearable and Ubiquitous Technologies*, 5(3):1–22, 2021.

[37] S. Gupta, D. Morris, S. Patel, and D. Tan. Soundwave: using the doppler effect to sense gestures. In *Proceedings of the SIGCHI Conference on Human Factors in Computing Systems*, pages 1911–1914, 2012.

[38] U. Ha, S. Assana, and F. Adib. Contactless seismocardiography via deep learning radars. In *Proceedings of the 26th annual international conference on mobile computing and networking*, pages 1–14, 2020.

[39] G. He, S. Chen, D. Xu, X. Chen, Y. Xie, X. Wang, and D. Fang. Fusang: Graph-inspired robust and accurate object recognition on commodity mmwave devices. In *Proceedings of the 21st Annual International Conference on Mobile Systems, Applications and Services*, pages 489–502, 2023.

[40] K. He, X. Zhang, S. Ren, and J. Sun. Deep residual learning for image recognition. In *Proceedings of the IEEE conference on computer vision and pattern recognition*, pages 770–778, 2016.

[41] V. Hers, D. Corbugy, I. Joslet, P. Hermant, J. Demarteau, B. Delhougne, G. Vandermoten, and J. Hermanne. New concept using passive infrared (pir) technology for a contactless detection of breathing movement: a pilot study involving a cohort of 169 adult patients. *Journal of clinical monitoring and computing*, 27:521–529, 2013.

[42] D. Huang, R. Nandakumar, and S. Gollakota. Feasibility and limits of wi-fi imaging. In *Proceedings of the 12th ACM conference on embedded network sensor systems*, pages 266–279, 2014.

[43] T. Iizuka, T. Sasatani, T. Nakamura, N. Kosaka, M. Hisada, and Y. Kawahara. Millisign: mmwave-based passive signs for guiding uavs in poor visibility conditions. In *Proceedings of the 29th Annual International Conference on Mobile Computing and Networking*, pages 1–15, 2023.

[44] S. M. Islam, O. Boric-Lubecke, V. M. Lubecke, A.-K. Moadi, and A. E. Fathy. Contactless radar-based sensors: Recent advances in vital-signs monitoring of multiple subjects. *IEEE Microwave Magazine*, 23(7):47–60, 2022.

[45] S. M. Islam, N. Motoyama, S. Pacheco, and V. M. Lubecke. Non-contact vital signs monitoring for multiple subjects using a millimeter wave fmcw automotive radar. In *2020 IEEE/MTT-S International Microwave Symposium (IMS)*, pages 783–786. IEEE, 2020.

[46] S. S. Jayaweera, B. Wang, X. Zeng, W.-H. Wang, and K. R. Liu. Wifi-based robust child presence detection for smart cars. In *ICASSP 2023-2023 IEEE International Conference on Acoustics, Speech and Signal Processing (ICASSP)*, pages 1–5. IEEE, 2023.

[47] J. Jung, S. Lim, B.-K. Kim, and S. Lee. Cnn-based driver monitoring using millimeter-wave radar sensor. *IEEE Sensors Letters*, 5(3):1–4, 2021.

[48] A. Kajiwara. Circular polarization diversity with passive reflectors in indoor radio channels. *IEEE Transactions on Vehicular technology*, 49(3):778–782, 2000.

[49] A. Karaman, A. S. Z. Tan, B. Li, L. G. H. Thien, R. X. Yong, S. Qie, and Y. Yao. Thermsafe: Child heat injury prevention in heated locked cars, 2017.

[50] F. Khan, S. Azou, R. Youssef, P. Morel, and E. Radoi. Ir-uwb radar-based robust heart rate detection using a deep learning technique intended for vehicular applications. *Electronics*, 11(16):2505, 2022.

[51] S. Kianoush, S. Savazzi, F. Vicentini, V. Rampa, and M. Giussani. Device-free rf human body fall detection and localization in industrial workplaces. *IEEE Internet of Things Journal*, 4(2):351–362, 2016.

[52] T. Kitamura, T. Kumagai, T. Takei, I. Matsushima, N. Oishi, and K. Suwa. Occupant body imaging based on occupancy grid mapping. In *2021 IEEE Intelligent Vehicles Symposium (IV)*, pages 755–761. IEEE, 2021.

[53] M. Lam, L. Dodds, A. Eid, J. Hester, and F. Adib. 3d self-localization of drones using a single millimeter-wave anchor. *arXiv preprint arXiv:2310.08778*, 2023.

[54] A. Lazaro, D. Girbau, and R. Villarino. Analysis of vital signs monitoring using an ir-uwb radar. *Progress In Electromagnetics Research*, 100:265–284, 2010.

[55] S.-Y. Lee, J.-H. Lee, H. Jang, and W. Lee. A framework for detecting the presence of an unattended child in a vehicle. In *2020 International SoC Design Conference (ISOCC)*, pages 59–60, 2020.

[56] S. K. Leem, F. Khan, and S. H. Cho. Vital sign monitoring and mobile phone usage detection using ir-uwb radar for intended use in car crash prevention. *Sensors*, 17(6):1240, 2017.

[57] W. Li, Y. Gao, Z. Hu, N. Liu, K. Wang, and S. Niu. In-vehicle occupant detection system using mm-wave radar. In *2022 7th International Conference on Communication, Image and Signal Processing (CCISP)*, pages 395–399. IEEE, 2022.

[58] W. Li, Y. Gao, Z. Hu, N. Liu, K. Wang, and S. Niu. In-vehicle occupant detection system using mm-wave radar. In *2022 7th International Conference on Communication, Image and Signal Processing (CCISP)*, pages 395–399. IEEE, 2022.

[59] X. Li, Y. He, and X. Jing. A survey of deep learning-based human activity recognition in radar. *Remote Sensing*, 11(9):1068, 2019.

[60] Y. Li, C. Gu, and J. Mao. An in-vehicle occupant detection technique based on a 60 ghz fmcw mimo radar. In *2022 IEEE MTT-S International Wireless Symposium (IWS)*, volume 1, pages 1–3. IEEE, 2022.

[61] Y. Li, X. Tian, T. Liu, and D. Tao. Multi-task model and feature joint learning. In *Twenty-fourth international joint conference on artificial intelligence*, 2015.

[62] Z. Li, T. Jin, Y. Dai, and Y. Song. Motion-robust contactless heartbeat sensing using 4d imaging radar. *IEEE Transactions on Instrumentation and Measurement*, 2023.

[63] J. Lian, J. Lou, L. Chen, and X. Yuan. Echospot: Spotting your locations via acoustic sensing. *Proceedings of the ACM on Interactive, Mobile, Wearable and Ubiquitous Technologies*, 5(3):1–21, 2021.

[64] P. Liaw, R. Y. Moon, A. Han, and J. D. Colvin. Infant deaths in sitting devices. *Pediatrics*, 144(1), 2019.

[65] Y. Ma, Y. Zeng, and V. Jain. Carosense: Car occupancy sensing with the ultra-wideband keyless infrastructure. *Proceedings of the ACM on Interactive, Mobile, Wearable and Ubiquitous Technologies*, 4(3):1–28, 2020.

[66] S. Mahmud, K. Li, G. Hu, H. Chen, R. Jin, R. Zhang, F. Guimbretière, and C. Zhang. Posesonic: 3d upper body pose estimation through egocentric acoustic sensing on smartglasses. *Proceedings of the ACM on Interactive, Mobile, Wearable and Ubiquitous Technologies*, 7(3):1–28, 2023.

[67] M. M. Moussa, R. Shoitan, Y.-I. Cho, and M. S. Abdallah. Visual-based children and pet rescue from suffocation and incidence of hyperthermia death in enclosed vehicles. *Sensors*, 23(16), 2023.

[68] P. Pathak, W. Burnside, and R. Marhefka. A uniform gtd analysis of the diffraction of electromagnetic waves by a smooth convex surface. *IEEE Transactions on antennas and propagation*, 28(5):631–642, 1980.

[69] A. Pearce, J. A. Zhang, R. Xu, and K. Wu. Multi-object tracking with mmwave radar: A review. *Electronics*, 12(2):308, 2023.

[70] V. Perrot, M. Polichetti, F. Varray, and D. Garcia. So you think you can das? a viewpoint on delay-and-sum beamforming. *Ultrasonics*, 111:106309, 2021.

[71] A. Qi, M. Ma, Y. Luo, G. Fernandes, G. Shi, J. Fan, Y. Qi, and J. Ma. Wise: Wireless intelligent sensing for human-centric applications. *IEEE Wireless Communications*, 2022.

[72] K. Qian, C. Wu, F. Xiao, Y. Zheng, Y. Zhang, Z. Yang, and Y. Liu. Acousticardiogram: Monitoring heartbeats using acoustic signals on smart devices. In *IEEE INFOCOM 2018-IEEE conference on computer communications*, pages 1574–1582. IEEE, 2018.

[73] M. S. Raheel, J. Coyte, F. Tubbal, R. Raad, P. Ogunbona, C. Patterson, and D. Perlman. Breathing and heartrate monitoring system using ir-uwb radar. In *2019 13th International Conference on Signal Processing and Communication Systems (ICSPCS)*, pages 1–5, 2019.

[74] Y. Rahmat-Samii. Reflector antennas. In *Antenna Handbook: Theory, Applications, and Design*, pages 949–1072. Springer, 1988.

[75] Y. Rong, I. Lenz, and D. W. Bliss. Vital signs detection based on high-resolution 3-d mmwave radar imaging. In *2022 IEEE International Symposium on Phased Array Systems & Technology (PAST)*, pages 1–6. IEEE, 2022.

[76] A. Rowden. What is a normal respiratory rate based on your age?, 2023.

[77] V. Selvaraju, N. Spicher, J. Wang, N. Ganapathy, J. M. Warnecke, S. Leonhardt, R. Swaminathan, and T. M. Deserno. Continuous monitoring of vital signs using cameras: A systematic review. *Sensors*, 22(11):4097, 2022.

[78] H. Shanbhag, S. Madani, A. Isanaka, D. Nair, S. Gupta, and H. Hassanieh. Contactless material identification with millimeter wave vibrometry. In *Proceedings of the 21st Annual International Conference on Mobile Systems, Applications and Services*, pages 475–488, 2023.

[79] D. Solomitckii, M. Heino, S. Buddappagari, M. A. Hein, and M. Valkama. Radar scheme with raised reflector for nlos vehicle detection. *IEEE Transactions on Intelligent Transportation Systems*, 23(7):9037–9045, 2021.

[80] H. Song, Y. Yoo, and H.-C. Shin. In-vehicle passenger detection using fmcw radar. In *2021 International Conference on Information Networking (ICOIN)*, pages 644–647. IEEE, 2021.

[81] H. Song, Y. Yoo, and H.-C. Shin. In-vehicle passenger detection using fmcw radar. In *2021 International Conference on Information Networking (ICOIN)*, pages 644–647, 2021.

[82] Y. Su, F. Zhang, K. Niu, T. Wang, B. Jin, Z. Wang, Y. Jiang, D. Zhang, L. Qiu, and J. Xiong. Embracing distributed acoustic sensing in car cabin for children presence detection. *Proceedings of the ACM on Interactive, Mobile, Wearable and Ubiquitous Technologies*, 8(1):1–28, 2024.

[83] N. Sulaiman, K. H. Ghazali, M. S. Jadin, A. A. Hadi, M. S. Najib, M. S. M. Zain, F. A. Halim, S. M. Daud, N. Zahed, and A. A. Abdullah. Development of comprehensive unattended child warning and feedback system in vehicle. In *MATEC Web of Conferences*, volume 90, page 01008. EDP Sciences, 2017.

[84] E. Tavanti, A. Rizik, A. Fedeli, D. D. Caviglia, and A. Randazzo. A short-range fmcw radar-based approach for multi-target human-vehicle detection. *IEEE Transactions on Geoscience and Remote Sensing*, 60:1–16, 2021.

[85] M. van Gastel, S. Stuijk, S. Overeem, J. P. van Dijk, M. M. van Gilst, and G. de Haan. Camera-based vital signs monitoring during sleep–a proof of concept study. *IEEE journal of biomedical and health informatics*, 25(5):1409–1418, 2020.

[86] P. Visconti, R. de Fazio, P. Costantini, S. Miccoli, and D. Cafagna. Innovative complete solution for health safety of children unintentionally forgotten in a car: a smart arduino-based system with user app for remote control. *IET Science, Measurement & Technology*, 14(6):665–675, 2020.

[87] A. Wang and S. Gollakota. Millisonic: Pushing the limits of acoustic motion tracking. In *Proceedings of the 2019 CHI Conference on Human Factors in Computing Systems*, pages 1–11, 2019.

[88] A. Wang, D. Nguyen, A. R. Sridhar, and S. Gollakota. Using smart speakers to contactlessly monitor heart rhythms. *Communications biology*, 4(1):1–12, 2021.

[89] F. Wang, X. Zeng, C. Wu, B. Wang, and K. R. Liu. Driver vital signs monitoring using millimeter wave radio. *IEEE Internet of Things Journal*, 9(13):11283–11298, 2021.

[90] F. Wang, F. Zhang, C. Wu, B. Wang, and K. R. Liu. Vimo: Multiperson vital sign monitoring using commodity millimeter-wave radio. *IEEE Internet of Things Journal*, 8(3):1294–1307, 2020.

[91] J. Wang, L. Gao, X. Yuan, and L. Liu. A seat occupancy detection system using millimeter wave radar. In *Proceedings of the 2022 5th International Conference on Telecommunications and Communication Engineering*, pages 95–99, 2022.

[92] Y. Wang. Tesla Adopts Interior Radar for Interior Monitoring. *IDTechEx*, Feb. 2024.

[93] C. Will, P. Vaishnav, A. Chakraborty, and A. Santra. Human target detection, tracking, and classification using 24-ghz fmcw radar. *IEEE Sensors Journal*, 19(17):7283–7299, 2019.

[94] D. T. Wisland, K. Granhaug, J. R. Pleym, N. Andersen, S. Støa, and H. A. Hjortland. Remote monitoring of vital signs using a cmos uwb radar transceiver. In *2016 14th IEEE International New Circuits and Systems Conference (NEWCAS)*, pages 1–4. IEEE, 2016.

[95] Y. Wu, H. Ni, C. Mao, J. Han, and W. Xu. Non-intrusive human vital sign detection using mmwave sensing technologies: A review. *ACM Transactions on Sensor Networks*, 20(1):1–36, 2023.

[96] M. Xiang, W. Ren, W. Li, Z. Xue, and X. Jiang. High-precision vital signs monitoring method using a fmcw millimeter-wave sensor. *Sensors*, 22(19):7543, 2022.

[97] H. Xue, Q. Cao, C. Miao, Y. Ju, H. Hu, A. Zhang, and L. Su. Towards generalized mmwave-based human pose estimation through signal augmentation. In *Proceedings of the 29th Annual International Conference on Mobile Computing and Networking*, pages 1–15, 2023.

[98] H. Xue, Y. Ju, C. Miao, Y. Wang, S. Wang, A. Zhang, and L. Su. mmmesh: Towards 3d real-time dynamic human mesh construction using millimeter-wave. In *Proceedings of the 19th Annual International Conference on Mobile Systems, Applications, and Services*, pages 269–282, 2021.

[99] M. Yang, X. Yang, L. Li, and L. Zhang. In-car multiple targets vital sign monitoring using location-based vmd algorithm. In *2018 10th International Conference on Wireless Communications and Signal Processing (WCSP)*, pages 1–6. IEEE, 2018.

[100] Z. Yang, M. Bocca, V. Jain, and P. Mohapatra. Contactless breathing rate monitoring in vehicle using uwb radar. In *Proceedings of the 7th international workshop on real-world embedded wireless systems and networks*, pages 13–18, 2018.

[101] Z. Yang, P. H. Pathak, Y. Zeng, X. Liran, and P. Mohapatra. Vital sign and sleep monitoring using millimeter wave. *ACM Transactions on Sensor Networks (TOSN)*, 13(2):1–32, 2017.

[102] X. Zeng, B. Wang, C. Wu, S. D. Regani, and K. R. Liu. Intelligent wi-fi based child presence detection system. In *ICASSP 2022-2022 IEEE International Conference on Acoustics, Speech and Signal Processing (ICASSP)*, pages 11–15. IEEE, 2022.

[103] X. Zeng, B. Wang, C. Wu, S. D. Regani, and K. R. Liu. Wicpd: Wireless child presence detection system for smart cars. *IEEE Internet of Things Journal*, 9(24):24866–24881, 2022.

[104] Y. Zeng, D. Wu, J. Xiong, J. Liu, Z. Liu, and D. Zhang. Multisense: Enabling multi-person respiration sensing with commodity wifi. *Proceedings of the ACM on Interactive, Mobile, Wearable and Ubiquitous Technologies*, 4(3):1–29, 2020.

[105] Y. Zeng, D. Wu, J. Xiong, E. Yi, R. Gao, and D. Zhang. Farsense: Pushing the range limit of wifi-based respiration sensing with csi ratio of two antennas. *Proceedings of the ACM on Interactive, Mobile, Wearable and Ubiquitous Technologies*, 3(3):1–26, 2019.

[106] I. P. O. V. ZERO. Euro ncap 2025 roadmap. 2017.

[107] Y. Zhang, W. Hou, Z. Yang, and C. Wu. {VeCare}: Statistical acoustic sensing for automotive {In-Cabin} monitoring. In *20th USENIX Symposium on Networked Systems Design and Implementation (NSDI 23)*, pages 1185–1200, 2023.

[108] T. Zheng, Z. Chen, C. Cai, J. Luo, and X. Zhang. V2ifi: In-vehicle vital sign monitoring via compact rf sensing. *Proceedings of the ACM on Interactive, Mobile, Wearable and Ubiquitous Technologies*, 4(2):1–27, 2020.